Normal stress differences in Non-Brownian fibre suspensions

S.BOUNOUA[a], P.KUZHIR[a], E.LMAIRE[a]

a. LPMC, Nahed-Sihem.BOUNOUA@unice.fr, Pavel.KUZHIR@unice.fr, Elisabeth.LEMAIRE@unice.fr

Résumé :

Nous presentons une étude expérimentale des différences de contrainte normale dans les suspensions de fibres rigides non-browniennes. La première et la seconde différence de contrainte normale sont mesurées au cours d'une même expérience qui consiste à déterminer le profil radial de la seconde contrainte normale, Σ_{22}, dans un écoulement torsionnel plan-plan. De ce profil, sont extraites les valeurs des deux différences de contraintes normales. Les suspensions que nous avons étudiées sont constituées de fibres monodisperses suspendues dans un fluide newtonien de même densité. Deux longueurs de fibres et trois rapports d'aspect ont été testés. Une large gamme de concentrations a été étudiée, permettant d'explorer les trois régimes de concentration : dilué, semi-dilué et concentré. Les résultats montrent que N_1 est positive tandis que N_2 est négative. Leurs valeurs augmentent quand le paramètre nL^2d augmente (n représente le nombre de fibres par unité de volume, L la longueur des fibres et d leur diamètre). La valeur absolue de N_2 est environ deux fois plus faible que N_1, ce qui contredit les prédictions de [Shaqfeh and Fredrickson, 1990] selon lesquelles $N_2 = -\frac{1}{7}N_1$ mais est en bon accord avec les résultats numériques récents de [Snook et al., 2014]

Abstract :

In this paper, we present an experimental study of the normal stress differences that arise in non-Brownian rigid fibre suspensions subject to a shear flow. The first and the second normal stress differences are measured using a single experiment which consists of determining the radial profile of the second normal stress, along the velocity gradient direction, Σ_{22}, in a torsional flow between two parallel discs. Suspensions are made of monodispersed fibres immersed a neutrally buoyant Newtonian fluid. Two lengths and three aspect ratios of the fibers and a wide range of concentrations have been tested. N_1 is found to be positive while N_2 is negative and the magnitude of both normal stress differences increases when nL^2d increases (n is the number of fibres per unite volume, L, the fibre length and d, their diameter). The magnitude of N_2 is found to smaller than N_1, but not negligible, which is in contradiction with the theoretical prediction of [Shaqfeh and Fredrickson, 1990] in which they predicted that $N_2 = -\frac{1}{7}N_1$ but consistent with the recent numerical work of [Snook et al., 2014].

Mots clefs : Fibre Suspension, rheology, Normal stress differences

1 Introduction

Fibre suspension rheology is involved in many industrial processes that make use of the reinforcement of polymeric materials with short fibres. This is a rather complicated question since there is a strong coupling between the flow, the fibre orientation and the rheological properties. Furthermore besides these conceptual difficulties, experimental measurements of the rheological properties and especially normal stress differences are tricky and only few results are available in literature [Petrich et al., 2000], [Sepehr et al., 2004], [Snook et al., 2014], [Keshtkar et al., 2009]. Actually, in most studies [Petrich et al., 2000], [Sepehr et al., 2004],

[Keshtkar et al., 2009] it is the difference between the first and the second normal stress differences, $N_1 - N_2$ that is measured. Indeed, usually a parallel plate geometry is used and $N_1 - N_2$ is directly determined from the measurement of the net thrust force exerted on one of the disks. Then N_2 is commonly assumed to be much smaller than N_1 so that the measurement of the thrust force is expected to give a rough value of N_1. Recently, [Snook et al., 2014] have determined independently N_1 and N_2 from measuring the deformation of the free surface of fibre suspensions flowing in a tilted trough and in a Weissenberg rheometer and have shown that the magnitude of the first normal stress difference which is positive is only approximately twice that of the second normal stress difference which is negative. In this paper, we present normal stress measurements that have been carried out with an original device, previously designed by [Dbouk, 2011] in order to measure both N_1 and N_2 in suspensions of spherical particles. The measurements are carried out for neutrally buoyant suspensions made of short (rigid) fibres dispersed a Newtonian fluid for concentrations ranging from 0.03 to 0.25, 3 aspect ratios and 2 fibre lengths. The measurement principle is described in section 2 and details on fibre suspensions and experimental device are given in section 3. Results are presented and discussed in the last section of the paper.

2 Material function in parallel-plate geometry

2.1 Definition of material function in parallel-plate geometry

We consider a suspension of rigid rod-like particles immersed in a Newtonian fluid characterized by its viscosity $\eta_s(\phi)$ which depends on the fibre volume fraction ϕ and subject to a shear stress Σ_{12} in torsional flow between two parallel plates, where the indices 1 and 2 denote the direction of the shear velocity and of the velocity gradient respectively.

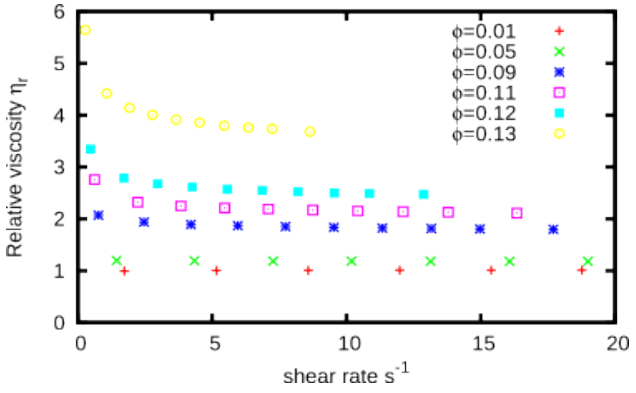

Figure 1: Typical behaviour of the shear viscosity versus the shear rate of fibre suspensions for different concentrations. For low concentrations, the suspensions exhibit a Newtonian behaviour, while, for the largest concentrations, the suspensions are shear-thinning and, as the concentration increases, the shear-thinning behaviour becomes more pronounced.

Since fibre suspensions exhibit a shear thinning behaviour when increasing the volume fraction of fibres, one has to define the rheological law as :

$$\Sigma_{12} = \eta_s(\phi)\dot{\gamma}^n \tag{1}$$

Where n is the shear-thinning index and $n \leq 1$. In figure (1) we report the behaviour of the relative viscosity $\eta_r = \dfrac{\eta_s(\phi)}{\eta_0}$, where η_0 is the viscosity of the suspending fluid, as a function of the shear rate $\dot{\gamma}$.
It is known that at high volume fraction of fibres in suspension, anisotropic normal stresses appear Σ_{11}, Σ_{22}

and Σ_{33} where the index 3 denotes the direction of the vorticity. Then, two important quantities are introduced : the first and the second normal stress differences defined as :

$$N_1(\dot{\gamma}) = \Sigma_{11} - \Sigma_{22} \quad , \quad N_2(\dot{\gamma}) = \Sigma_{22} - \Sigma_{33} \tag{2}$$

Which are known to scale linearly with the shear stress $N_i(\dot{\gamma}) \propto \Sigma_{12}$ where $i = 1, 2$. Hence we introduce the first and the second normal stress coefficients $\alpha_1(\phi)$ and $\alpha_2(\phi)$:

$$N_1(\dot{\gamma}) = -\alpha_1(\phi)\Sigma_{12} \quad , \quad N_2(\dot{\gamma}) = -\alpha_2(\phi)\Sigma_{12} \tag{3}$$

The negative sign is set according to a commonly used convention when the normal stresses are compressional. These quantities $\eta(\phi)$, $\alpha_1(\phi)$ and $\alpha_2(\phi)$ are called material functions which reflect the rheological behaviour of fibre suspensions.

2.2 Normal stress differences determination

Here we present the method to determine the values of the first and the second normal stress coefficients. We proceed by the determination of the radial profile of the normal stress along the direction of the velocity gradient Σ_{22}, in a torsional flow between tow parallel discs separated by a distance h. The flow is generated by a torque Γ applied to the upper disc that rotates with an angular velocity, Ω. The shear rate $\dot{\gamma}(r) = \dfrac{\partial v}{\partial z}$ depends linearly on r.
In our experiment, we consider only the case of laminar flow. The suspending fluid is prepared in such a way that the viscous forces dominate the inertial forces. We ensure that for the highest applied torque Γ , the Reynolds Number (Inertial forces/ Viscous forces) remains sufficiently small:

$$N_{Re} = \frac{\rho \Omega R h}{\eta} \ll 1 \tag{4}$$

In this geometry the components of the suspension velocity are

$$v_\theta(r) = r\Omega(z) \quad , v_r = 0 \quad , v_z = 0 \tag{5}$$

and the shear rate is :

$$\dot{\gamma}(r) = \frac{\Omega r}{h} \tag{6}$$

Starting from the equation of motion (**Stockes equation**) in cylindrical coordinates which takes the form

$$r - component \qquad \frac{\partial \Sigma_{33}}{\partial r} + \frac{\Sigma_{33} - \Sigma_{11}}{r} = 0 \tag{7}$$

$$\theta - component \qquad \frac{\partial \Sigma_{12}}{\partial z} = 0 \tag{8}$$

and from equation (2) and (3) we express Σ_{11} and Σ_{33} in terms of of N_1, N_2 and Σ_{22}, we obtain the radial profile of the second normal stress Σ_{22}.

$$\frac{\partial \Sigma_{22}}{\partial r/R} = -\eta_s \dot{\gamma}_R^n \left(\frac{\alpha_1 + (n+1)\alpha_2}{n} \left(\frac{r}{R} \right)^{n-1} \right) \tag{9}$$

Where $\dot{\gamma}(R)$ is the shear rate at the rim $\dot{\gamma}(r = R) = \dfrac{\Omega R}{h}$. After integrating equation (9) and assuming that at the $air/suspension$ interface, $\Sigma_{33}(R)$ is the sum of capillary and atmospheric pressure :

$$\Sigma_{33}(r = R) = P_{Cap} + P_{atm} = P_{ref} \tag{10}$$

We obtain the expression of Σ_{22} :

$$\Sigma_{22}(r/R) = -\eta_s \dot{\gamma}_R^n \left(\underbrace{\frac{\alpha_1 + (n+1)\alpha_2}{n}}_{Slope \quad A} \left(\frac{r}{R}\right)^n - \underbrace{\frac{\alpha_1 + \alpha_2}{n}}_{ordinate \quad at \quad origin \quad B} \right) + P_{ref} \tag{11}$$

And P_{ref} is set to zero. Equation (11) shows that the radial profile of the second normal stress Σ_{22} is expected to vary linearly when Σ_{22} is plotted against $(r/R)^n$. Then, from a linear combination of the slope, A, and the ordinate at the origin, B, the value of the two normal stress coefficients $\alpha_1(\phi)$ and $\alpha_2(\phi)$ can be deduced.

$$\begin{cases} \alpha_1(\phi) = -A - (1+n)B \\ \\ \alpha_2(\phi) = A + B \end{cases} \tag{12}$$

3 Experiment

3.1 Preparation of fibres suspensions

The suspensions that we have studied are made of mono-disperse fibres of polyamide provided by La Societe Nouvelle Le Flockage, dispersed in a Newtonian fluid which is a mixture of pure water, zinc bromide and Uncoil UNCON $75H90000$.
In order to avoid any sedimentation or flotation effect, the suspending medium is prepared to have the same density as the fibres. The fibre length L and diameter d were specified by the society and their values have been verified by optical microscopy. In our experiment different fibre aspect ratios and lengths have been investigated. We have prepared a series of fibre volume fractions in order to explore the three concentration regimes : (dilute, semi-dilute and concentrated regimes). After adding fibres in the suspending liquid, the suspension is gently mixed with a spatula. After that, the suspensions are put in closed flasks and placed in centrifuge and then in an ultrasonic for a period of $(2, 4)$ hours in order to eliminate air bubbles. The characteristics of fibre suspensions are reported in table 1.

Aspect ratio	Length $L(\mu)$	Diameter $d(\mu)$	density ρ g/cm^3	Concentration regime limit $\phi^{'} = 2\pi/r^2$	$\phi^{''} = \pi/r$
18	500	28	1.09	0.02	0.17
18	300	17	1.09	0.02	0.17
10	300	30	1.09	0.06	0.31
33	500	15	1.34	0.005	0.09

Table 1: Characteristics of fibre suspensions studied in our experiments. $\phi^{'} = 2\pi/r^2$ and $\phi^{''} = \pi/r$ denotes the characteristic volume fraction that separate the dilute regime from the semi dilute one and the semi-dilute regime from the concentrated one, respectively.

We consider Non-Brownian suspensions. The fibres are large enough for hydrodynamic forces to dominate Brownian forces as it is determined by the Peclet Number (Hydrodynamic forces / Brownian forces), $N_{Pe} = \frac{\dot{\gamma}}{D_r}$, where D_r is the rotary Brownian diffusion coefficient :

$$N_{Pe} = \frac{\eta_0 \dot{\gamma} \pi L^3}{3 k_B T \ln(r)} \sim 10^9 \gg 1 \tag{13}$$

3.2 Experimental device

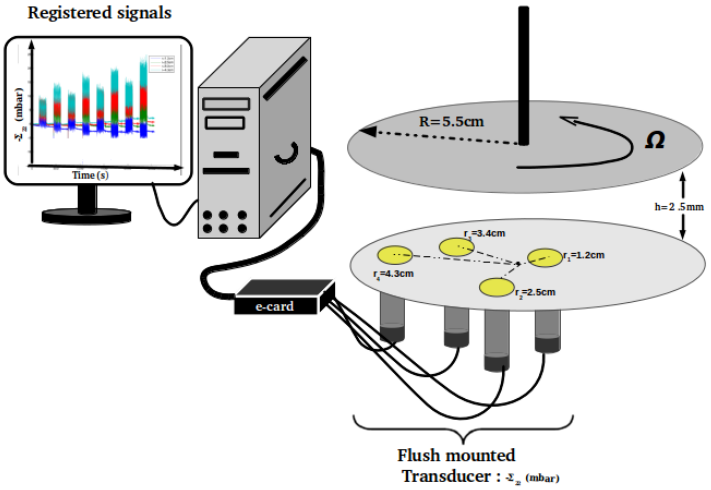

Figure 2: Experimental device used to perform pressure measurement in the direction of the velocity gradient Σ_{22}. The lower disc is equipped with fourth flash transducer placed at different radial position : ($r_1 = 1.2cm$, $r_2 = 2.5cm$, $r_3 = 3.4cm$ and $r_4 = 4.3cm$) and allowed to measure the total pressure in the suspension.

The Normal stress difference measurements are conducted using a controlled-stress rheometer *HAAKE MARSS II* in parallel plate geometry. The suspension is placed between tow parallel discs of radius $R = 5.5cm$ separated with distance $h \sim 2.5mm$. The lower disc is equipped with four flash mounted differential pressure transducers $(ATM \pm 25mbar, STS)$ and placed at different radial positions as shown in figure (2) that allowed to measure the total normal stress Σ_{22} of the suspension. With this sensor network we are able to determine the radial profile of Σ_{22} and then the two normal stress coefficients, $\alpha_1(\phi)$ and $\alpha_2(\phi)$, as explained in section (2.2). Note that great care must be taken in order to get a precise pressure measurement, if not, extra pressure will appear as hole pressure which are due to a misalignment of the transducers. In order to avoid these hole pressure effects, the pressure membrane transducer must be placed at the same level as the lower disc. Thus we adjust the level by coating the surface of transducers with paraffin. After all the necessary calibration, we have verified the validity of the pressure measurements. The transducer responses are tested by measuring the hydrostatic pressure of a liquid column and also the inertial pressure as detailed in [Dbouk, 2011]

3.3 Experimental procedure

To begin our experiment, we carefully place on the lower disc the suspension in order to prevent air bubble formation then we place a drop of suspension on the upper disc and bring it down slowly to reach a gap width of $2.5mm$ and wait until the suspension is spread completely across the gap width. Then the upper disc is raised by 50μ, and the extra of the suspension is carefully cleaned. After that, all the transducers are set to zero.

The experimental protocol is shown in figure (3). We applied a series of torque Γ in the clockwise and counter-clockwise directions with a period T_{shear}. Since we aim to measure normal stress difference in the steady state regime i.e. when the fibre orientation is steady. The run time, T_{shear}, is chosen to be grater than five times the Jeffrey period [Jeffery, 1922] reached at the rim $T_J = \dfrac{2\pi}{\dot{\gamma}(R)} \times \left(\frac{1}{r} + r\right)$.

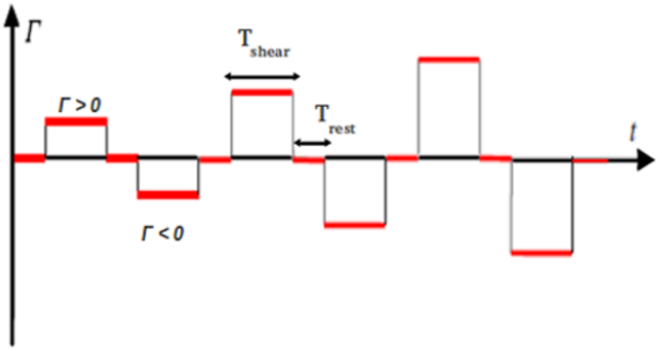

Figure 3: A series of the applied torque during the same period T_{shear} in the clockwise and counter-clockwise directions with a time rest T_{rest} between the tow directions.

Since the shear rate at the most central transducer is equal to : $\dot{\gamma}(r_1) = \frac{r_1}{R}\dot{\gamma}(R)$. With $r_1 = 1.2cm$ and $R = 5.5cm$, the fibres reach their steady orientation state at $T_J(r_1) \simeq 5 \times T_J(R)$. Furthermore, we ensure that the suspension shear viscosity η_s has attained a steady value during the run time T_{shear}.

Figure (4) shows an example of the registered signal over the run time. The normal stress Σ_{22} is obtained upon averaging the recorded signal over several revolutions in clockwise and counter-clockwise directions, this allowed to eliminate the parallelism defects between the rotating and the fixed discs. In our experiment the parallelism defect is about 60μ. If not corrected, this parallelism defect generates a pressure error, that is evaluated by [Dbouk, 2011] :

$$\delta p \simeq \eta\Omega R^2 \frac{\delta h}{h^3} = \Sigma_{12}\frac{\delta h R}{h^2} \tag{14}$$

Equation (14) shows that the error pressure is proportional to the shear stress and to the inverse of the gap width squared, so to reduce this effect, it will be judicious to work with a wide gap width.

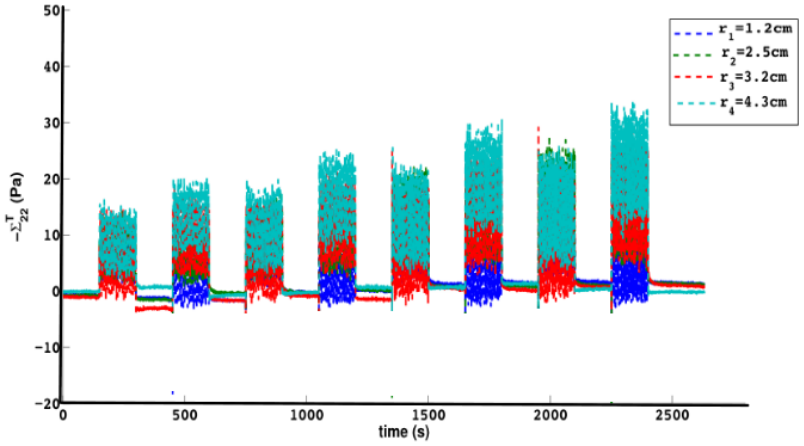

Figure 4: Example of the registered signals provided by the direct transducers situated at different radial positions r_i during a shear flow for a period T_{shaer} in the clockwise and counter-clockwise with a time rest T_{rest} between the two directions.

4 Results and discussion

Figure (5 a) Shows that, as expected from equation (11), when Σ_{22} is plotted against $(r/R)^n$, the profiles are linear and figure (5 b) indicates that, when Σ_{22} is rescaled with Σ_{12} , all profiles collapse.

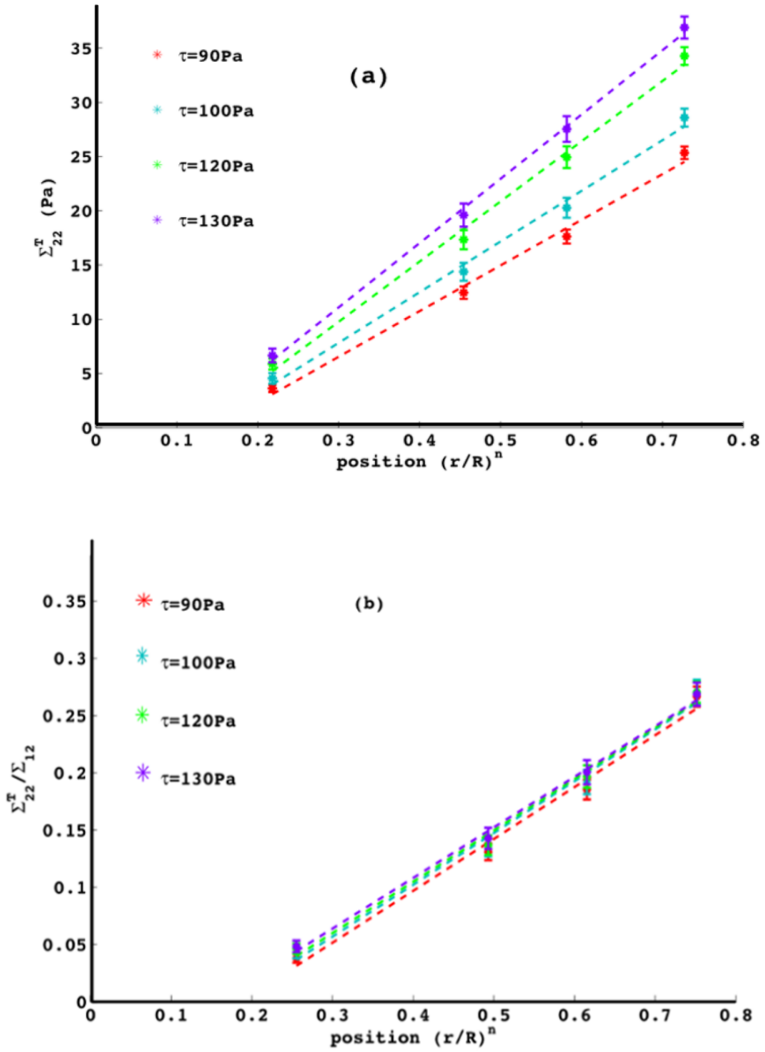

Figure 5: (a) Variation of the registered values of Σ_{22}, averaged over the clockwise and the anti-clockwise rotations with respect to the normalized radius, for different values of applied shear stresses at the rim, for fibre suspension with $\phi = 0.21$ and $r = 10$. (b) variation of the normalized $\frac{\Sigma_{22}}{\Sigma_{12}}$. All the measured pressures at a given position collapse. The value of $\alpha_1(\phi)$ and $\alpha_2(\phi)$ are deduced from the slope and the ordinate at the origin of the mean normalized profile.

Then $\alpha_1(\phi)$ and $\alpha_2(\phi)$ are extracted from the mean normalized profile and results are given on figures (6). Whatever the length or the aspect ratio of the fibres, N_1 appears to be almost a function of only nL^2d, at least in the dilute and semi-dilute regimes $nL^2d \leqslant$, whereas, for a given value of nL^2d, the magnitude of N_2 decreases as the aspect ratio increases.
Furthermore it worth to note that, contrarily to what is often assumed, N_2 is not negligible compared to N_1. The first normal stress differences are positive and approximately twice the magnitude of the second normal

stress differences (that are negative). This is consistent with the results of [Snook et al., 2014]. Nevertheless, we have measured much larger magnitudes of the normal stress differences than [Snook et al., 2014]. As demonstrated by a numerical study of the same authors, this difference should originate in the confinement that is present in our experiments and that acts to increase the number of contacts between fibres leading to higher values of the normal stress differences.

Figure (7) shows a comparison with previous experimental results of the literature, namely the results of [Petrich et al., 2000] that have been obtained for $r = 50$ and for various concentrations and those of [Keshtkar et al., 2009] obtained for r=35 and two fibre concentrations : 0.016 and 0.065. These last results

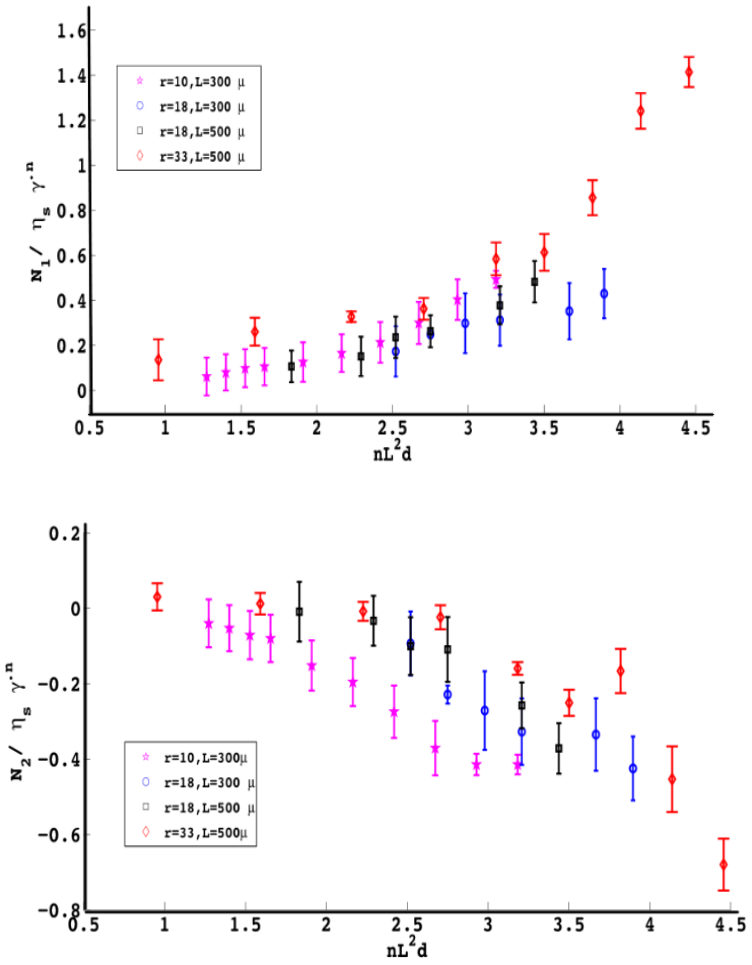

Figure 6: Up. First normal stress N_1 rescaled by the shear stress Σ_{12}. Down. Second normal stress N_2 rescaled by the shear stress Σ_{12} for different aspect ratio. Both value are plotted against nL^2d and clearly shows that N_1 and N_2 increase with nL^2d

can be directly compared with those we have obtained for $r = 33$ and the agreement is fairly good even though the confinement is not exactly the same in both experiments ($3L$ for [Keshtkar et al., 2009] and $5L$ for us).

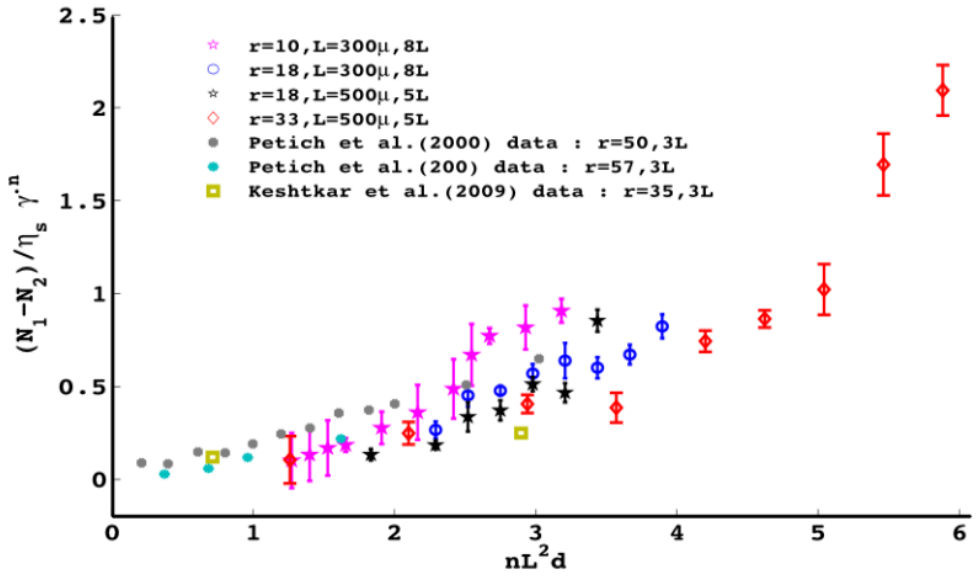

Figure 7: First normal stress difference $N_1 - N_2$ versus nL^2d Comparison of our results with those obtained by conventional method, our result are in a good agreement and confirm the non zero of the second normal stress difference N_2.

5 Conclusion

Both first and second normal stress differences have been measured for a large range of aspect ratios and fibre concentrations so that dilute, semi-dilute and concentrated regimes have been explored. The results show that $N_1 \sim -2N_2$. Further studies should be performed, in particular to explore from an experimental point of view the effect of confinement.

References

Talib Dbouk. *Rheology of concentrated suspensions and shear-induced migration*. Theses, Université Nice Sophia Antipolis, December 2011. URL `https://tel.archives-ouvertes.fr/tel-00673964`.

George B Jeffery. The motion of ellipsoidal particles immersed in a viscous fluid. *Proceedings of the Royal Society of London. Series A*, 102(715):161–179, 1922.

M Keshtkar, MC Heuzey, and PJ Carreau. Rheological behavior of fiber-filled model suspensions: effect of fiber flexibility. *Journal of Rheology (1978-present)*, 53(3):631–650, 2009.

Michael P Petrich, Donald L Koch, and Claude Cohen. An experimental determination of the stress–microstructure relationship in semi-concentrated fiber suspensions. *Journal of non-newtonian fluid mechanics*, 95(2):101–133, 2000.

Maryam Sepehr, Pierre J Carreau, Michel Moan, and Gilles Ausias. Rheological properties of short fiber model suspensions. *Journal of Rheology (1978-present)*, 48(5):1023–1048, 2004.

Eric SG Shaqfeh and Glenn H Fredrickson. The hydrodynamic stress in a suspension of rods. *Physics of Fluids A: Fluid Dynamics (1989-1993)*, 2(1):7–24, 1990.

Braden Snook, Levi M Davidson, Jason E Butler, Olivier Pouliquen, and Elisabeth Guazzelli. Normal stress differences in suspensions of rigid fibres. *Journal of Fluid Mechanics*, 758:486–507, 2014.